Optica Applicata Vol. XXIX, No 3, 1999

Superresolution phase image microscope

CHRISTIAAN VELZEL

Centre for Manufacturing Technology, Philips, Eindhoven, The Netherlands.

JAN MASAJADA

Institute of Physics, Wrocław University of Technology, Wybrzeże Wyspiańskiego 27, 50-370 Wrocław, Poland.

While reflecting a wave front from a rough surface we can find areas with multi-valued defined phase (the same phenomena are present when the wave front passes through inhomogeneous or rough object). These regions – singularities – have the specific features and may cause a number of interesting phenomena to occur. We can treat them as well defined physical beings. We can also try to set optical instruments based on the birth, propagation and detection of singularities. One of such instruments under development is superresolution phase image microscope (SUPHIM). In the paper, we present briefly some basic information on singularities. Next, we give some information about SUPHIM. We also show examples of the experimental results that have been taken with SUPHIM working prototype.

1. Introduction

The first well known criterion of resolution was proposed by Rayleigh. The next well known resolution criterion based on the spatial frequencies cut-off was derived from the Abbe theory of imaging. The resolution criteria of Rayleigh and Abbe fixed the classical limit of resolution. Every instrument exceeding this limit is recognized as super- or ultra-resolving.

From the very beginning a number of ideas have been put forward to overcome the classical resolution limit. As an example we would like to refer to papers by LUKOSZ [1]–[3]. He has suggested some other way of understanding the resolution limits. According to Lukosz, in the optical systems the number of degrees of freedom must be conserved. Sacrifying the resolution with respect to one variable (for example, field of view) we can exceed the resolution with respect to other ones (for example, spatial frequencies).

In the absence of noise there are possibilities to get much better resolution than it is defined by Rayleigh, Abbe or Lukosz criteria [4]. In fact, the noise is the main reason of the resolution limits. And all criteria listed above do not consider noise. COX and SHEPPARD [5] have defined the resolution limit starting with the formula for informational capacity of the optical channels. Then they added to the formula a factor describing noise of the optical system. This seems to be promising way to follow for searching the general theory of resolution. The last step in this research program might be connecting the resolution criteria with the second law of thermodynamics. Theory of resolution founded on the entropy concept could be sensitive not only for noise, but also for *a priori* information, which is an important part of the theory of modern superresolution instruments.

We would like to distinguish between instruments which exceeding the classical resolution limits, are still limited by other factor than noise (for example, Lukosz method is limited by frequency cut-off, but at the higher level than it results from Abbe criterion). In such a case we will say ultraresolution. The instruments in which resolution is limited by noise we will call superresolving. The example of working superresolving instruments is scanning near field optical microscopy [6]. The other example is SUPHIM. The SUPHIM microscope is based on the analysis of the singularities in the optical wave fronts. In the next section we want to give some basic information concerning wave singularities. The last section is devoted to the SUPHIM.

2. Phase singularities

The wave front can contain points or lines where it is not single-value defined. These singular points may be considered as separate physical beings within the wave front. A well known type of singularity is phase jump by π – edge singularity [7]. It appears when the part of the wave front is shifted by angle π against its other part. Other interesting kinds of singularities are screw and mixed (edge+screw) ones [7]. We want to explain a bit more the phenomena of screw singularities.

Screw singularities appear at the points where the phase is totally undetermined. That means that the imaginary and real parts of the complex amplitude have to meet the conditions [8]:

$$\mathrm{Re}\{E(x_s, y_s, z_s)\} = |E(x_s, y_s, z_s)|\cos\varphi(x_s, y_s, z_s) = 0, \tag{1a}$$

$$\mathrm{Im}\{E(x_S, y_S, z_S)\} = |E(x_S, y_S, z_S)|\sin\varphi(x_S, y_S, z_S) = 0. \tag{1b}$$

From the above conditions we can find that the light intensity at the singular point equals zero.

The wave front with screw singularity has a helical form (Fig. 1), [9]. When the helix is clockwise we define the sign of its topological charge as $+n$ (n – natural number), in the opposite case we have $-n$. Figure 1 shows the wave fronts with the screw singularity having topological charge (1 and 3, respectively).

The wave front with screw singularity carries a non-zero angular momentum L [10], which in quantum picture is equal to $\lambda\cdot\hbar$, where $\hbar$ is Planck constant divided by 2π. The non-zero angular momentum results in structural stability of the screw singularities. One can destroy such a structure if its angular momentum is passed to some other system [11]. The other possibility is to anihilate two singularities with opposite sign. The set of screw singularities sharing the same wave front shows some more (than anihilation) charge particle like behaviours [12]. We can, for example, observe the stable arrangements of two or four singularities with geometry corresponding to electrical dipols or quadrupoles, respectively.

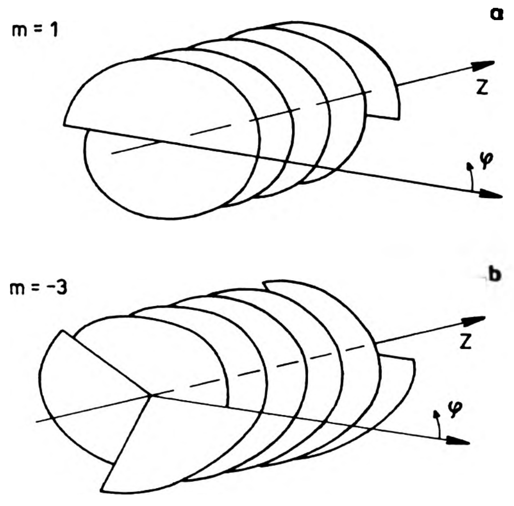

Fig. 1. Wave front with screw singularity of charge: +1 (a), −3 (b).

For the research purposes, the wave fronts with screw singularities can be generated by computer designed holograms [9], [11], [12]. The following equation describes (in polar coordinates) a Gaussian beam with singularity of charge m [9]

$$E(\rho,\varphi,z) = E_0\rho^m \exp(im\varphi)\exp(F_2(z)-\rho^2/F_1(z)) \tag{2}$$

where m corresponds to the value of the topological charge. Parameters $F_1(z)$ and $F_2(z)$ may be calculated by putting expression (2) into Helmholtz equation. Processing this equation leads to fringes pattern shown in Fig. 2.

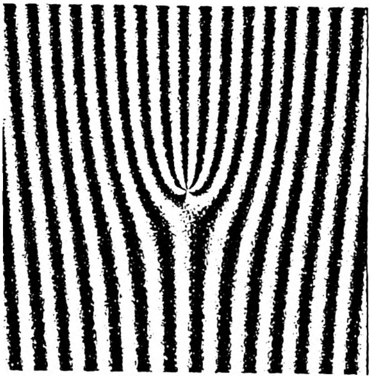

Fig. 2. Fringes geometry of the hologram generating wave front with the screw singularities of charge 5.

3. SUPHIM

At the moment there is no good theory of SUPHIM imaging. In this situation, we briefly present some ideas from the theory which shows that with SUPHIM like instrument we can get superresolution. Following the paper of BERTERO and PIKE [13] the relation between the object amplitude $v(x)$ and the image amplitude $u(x)$ can be written as:

$$u(x) = \int v(x')\,\mathrm{sinc}\left\{\frac{2\pi\sin\theta}{\lambda}(x-x')\right\}\mathrm{d}x'. \tag{3}$$

By expanding $v(x)$ in the eigenfunctions $g_i(x)$ of the operator acting on $v(x)$ in Eq. (3), *i.e.*, convolution by a function sinc, we get

$$v(x) = \sum_{i=1}^{\infty} a_i g_i(x, S). \tag{4}$$

Then image amplitude can be written

$$u(x) = \sum_{i=1}^{\infty} \lambda_i a_i g_i(x, S) \tag{5}$$

where: S is the classical number of degrees of freedom [14] defined as: $S = 2X\sin\theta/\lambda$, (X – size of the object domain, $\sin\theta$ – numerical aperture), λ_i is the eigenvalue belonging to the i-th eigenfunction. The eigenfunctions $g_i(x)$ are the linear prolate spheroidal functions [15], [16]. The value of λ_i for $i > S$ becomes very small. This means that in principle resolution beyond the classical limits is possible. In the real system the value of i is limited by the condition that $\lambda_i a_i$ is sufficiently larger than noise amplitude, so we have

$$u(x) = \sum_{i=1}^{K} \lambda_i a_i g_i(x) \tag{6}$$

where K is of the order of S [13].

According to this theory, the objects that can be described by eigenfunctions $g_i(x)$ with equal eigenvalues λ_i are reproduced identically in the image (4), (6). For two dimensions the number of objects that are imaged identically is greater, for instance, objects of the form

$$v(x, y) = a_k g_k(x, S_1) + b_j g_j(y, S_2) \tag{7}$$

are imaged identically when $\lambda_k(S_1) = \lambda_j(S_2)$.

Instead of looking for identical reproduction of the whole object we can require that only points of the object are reproduced identically where the modulus of v is zero. In this case, functions $g_i(x \text{ or } y)$ in (7) may correspond to different values of λ_i.

Suppose that the real and imaginary parts of $v(x, y)$ are given by:

$$\mathrm{Re}(v(x, y)) = a_k g_k(x), \tag{8a}$$

$$\mathrm{Im}(v(x, y)) = b_j g_j(y). \tag{8b}$$

Thus for the functions $g_k(x) = g_i(y) = 0$ we have a phase singularity (1). These singularities are reproduced in the image field. Equations (8) can be extended as follows:

$$\mathrm{Re}(v(x,y)) = \sum_k a_k g_k(x - x_k), \tag{9a}$$

$$\mathrm{Im}(v(x,y)) = \sum_j b_j g_j(y - y_j) \tag{9b}$$

where shifts x_k, y_j are chosen so that the eigenfunctions in the sum have a common zero. Then the singularity at this point is reproduced in the image field. Also the zero contours $\mathrm{Re}(v) = 0$ and $\mathrm{Im}(v) = 0$ are reproduced identically. We have taken the contours $\mathrm{Re}(v) = 0$ and $\mathrm{Im}(v) = 0$ perpendicular to each other. In the general two-dimensional theory this restriction would not be necessary.

The theory briefly presented above does not sufficiently explain the results obtained in the experiment. However, it shows that superresolution in the systems described below is possible. In [17], Tychinsky has reported an experiment with the system shown schematically in Fig. 3. In our system (Nanofocus GmbH, Duisburgh)

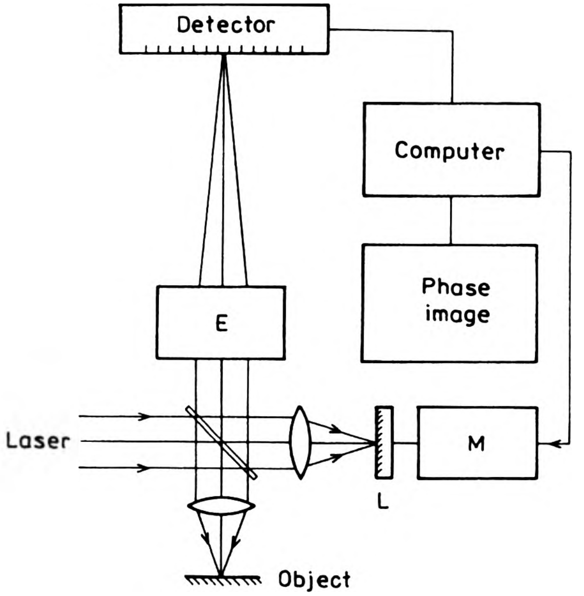

Fig. 3. Experimental setup (M — modulator, L — phase shift mirror, E — additional magnifying optics).

we used a modified interference microscope (Nomarski microscope produced by Leitz in Wetzlar, Germany). We added a laser illuminator. In the parallel laser beam that is directed by a neutral beam splitter to the objective we have placed an electrooptical modulator that produces a variable phase difference between the two polarization components of the illuminating wave. The illuminating wave is focused on the object by the objective lens, so that a small spot on the object is illuminated. This field reduction makes the superresolution easier. We also added a secondary magnification stage (40 ×) that images the diffraction spot on a CCD detector. In the primary image the diameter of the diffraction spot is about 50 μm. On the CCD detector the diameter becomes 2 mm. With a 50× objective one pixel of CCD detector corresponds to about 5 nm. The phase difference between the polarization components is measured by introducing the phase shift of 90°, 180°, 270°, 360° (by modulator) and processing the corresponding images with the image processing software (supplied by B. Breuckman GmbH).

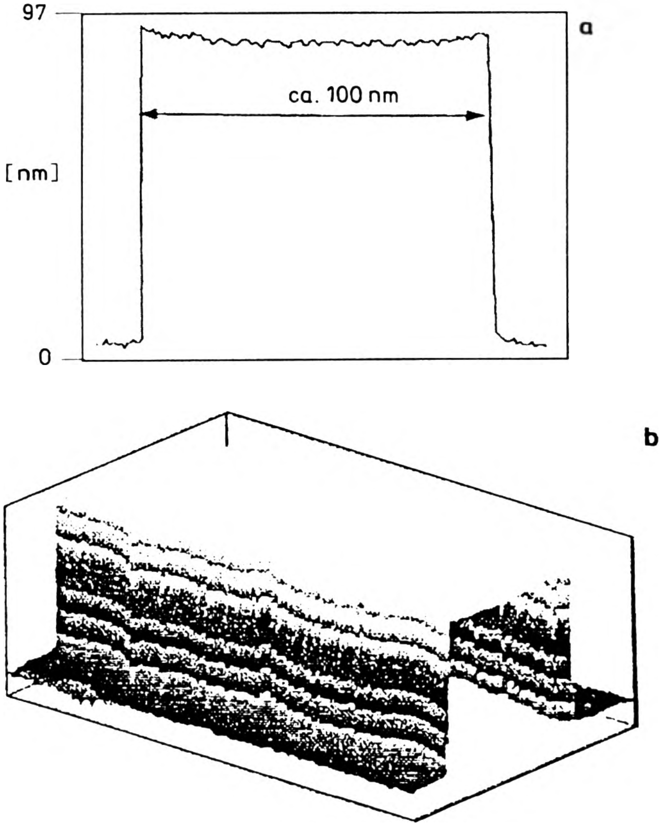

Fig. 4. Phase image (a) and profile (b) of the "line" object

As an example we present two phase images took by the setup described above. The first (Fig. 4) is a phase image of a line structure (photo-resist on silicon covered with thin gold layer) of 100 nm in width. The linewidth was checked by electron microscopy and AFM profile measurement. Figure 4 shows the pseudo-3D image and a cross-section. It is worth noting the steep slopes of the phase image, corresponding to an edge width of 3 pixels, *i.e.*, 15 nm on the object. Figure 5 shows the second phase image. The object consisted of small holes in a silicon surface. Independent measurements gave distance between the centres of two holes equal to 0.2 μm. The diameter of a single hole is smaller than 0.1 μm. In the phase image the number of holes is doubled. This means that periodic structures give artefacts in the phase image. Again the edges of the phase are very steep.

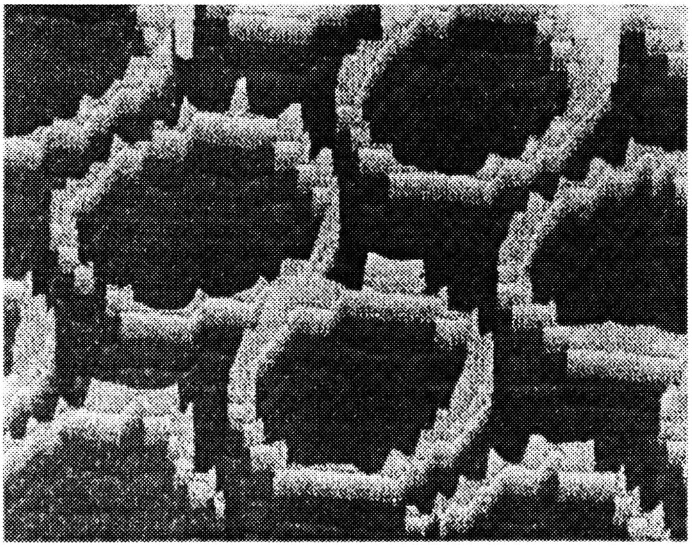

Fig. 5. Phase image of the periodic "dot" object.

From this result we can draw the following questions:

– Is the edge width shown in the phase image related to edge steepness in the object structure?

– What are the artefacts of general non-periodic structure?

– Why do phase images with magnification by 1000–10000 times (we have used also a special secondary magnification system $\times 250$) resemble so remarkably the object structures?

To resolve this and other questions some more study on the scattering of polarized light at submicron surface structures must be done.

4. Conclusions

The experiments of Tychinski, and those reported in this paper, show that noise-limited superresolution is possible and can be realised in interference microscopy. The present theory of superresolution cannot explain sufficiently superresolution phase image formation. For this reason further development of this kind of microscopy has to be supported by progress in theory of phase imaging.

References

[1] LUKOSZ W., J. Opt. Soc. Am. **56** (1966), 1463.
[2] LUKOSZ W., J. Opt. Soc. Am. **57** (1967), 932.
[3] BACHL A., LUKOSZ W., J. Opt. Soc. Am. **57** (1967), 163.
[4] Di FRANCIA T., Nuovo Cim., Suppl., **9** (1952), 426.
[5] COX I. J., SHEPPARD C. J. R., J. Opt. Soc. Am. A **3** (1986), 1152.
[6] COURJON D., VIGOUREUX J. M., SPAJER M., SARAYEDDINE K., LEBLANC S., , Appl. Opt. **29** (1990), 3734.

[7] NYE J. F., BERRY M. V., Proc. R. Soc. Lond. A **336** (1973), 165.
[8] FREUND I., SHVARTSMAN N., Phys. Rev. A **50** (1994), 5164.
[9] BAZHENOV V. YU. L., SOSKIN M. S., VASNETSOV M. U., J. Modern Opt. **39** (1992), 985.
[10] ALLEN L., BEIJERSBERGEN M. W., SPREEUW P. J., WOERDMAN J. P., Phys. Rev. A **45** (1992), 8185.
[11] HE H., FRIESE M. E. J., HECKENBERG N. R., RUBINSZTEIN-DUNLOP H., Phys. Rev. Lett. **75** (1995), 826.
[12] BASISTIY I. V., SOSKIN M. S., VASNETSOV M. V., Opt. Commun. **119** (1995), 604.
[13] BERTERO M., PIKE E. R., Opt. Acta **29** (1982), 727.
[14] PATERSON C., SMITH R., Opt. Commun. **124** (1996), 121.
[15] TORALDO DI FRANCIA, J. Opt. Soc. Am. **45** (1995), 497.
[16] SLEPIAN D., POLLAK H. O., Bell. Syst. Techn. J. **40** (1961), 43.
[17] TYCHINSKY V. P., Opt. Commun. **74** (1989), 41.

Received January 6, 1999